Supplement S3
APXS analysis of Funda

Extraformational sediment recycling on Mars

Kenneth S. Edgett, Steven G. Banham, Kristen A. Bennett, Lauren A. Edgar, Christopher S. Edwards, Alberto G. Fairén, Christopher M. Fedo, Deirdra M. Fey, James B. Garvin, John P. Grotzinger, Sanjeev Gupta, Marie J. Henderson, Christopher H. House, Nicolas Mangold, Scott M. McLennan, Horton E. Newsom, Scott K. Rowland, Kirsten L. Siebach, Lucy Thompson, Scott J. VanBommel, Roger C. Wiens, Rebecca M. E. Williams, and R. Aileen Yingst

APXS ANALYSIS OF FUNDA

To determine the composition of the pebble named Funda (**Fig. S3-1, plus Figs. 8C and 10 in main paper**), we used data acquired in a 4-position raster (**Fig. S3-1A**) by *Curiosity*'s Alpha Particle X-Ray Spectrometer (APXS) instrument (Gellert et al., 2015). The archived data files are listed in **Table S3-1**. We used methods described by Gellert et al. (2006), coupled with those developed by VanBommel et al. (2016), VanBommel et al. (2017), VanBommel et al. (2019a), and VanBommel et al. (2019b). Acquisition of data via a 4-point raster mitigated the effects of unavoidable millimeter-scale uncertainties (in three dimensions) in the placement of the APXS using the rover's robotic arm and allows for the deconvolution of distinct chemical end-members in the targeted area (VanBommel et al., 2016). The APXS field of view (FOV), when positioned such that its contact sensing plate is triggered, is 15 mm in diameter and increases as the distance between the instrument and the target increases (VanBommel et al., 2017). X-rays induced in the target material from within the FOV have a radial dependency and are highest at detector nadir; 50% of the induced X-rays originate from the innermost 16% of the FOV area (VanBommel et al., 2016). Thus, millimeter-scale changes in the position of the APXS, well within the accuracy of *Curiosity*'s robotic arm (Collins and Robinson, 2013), can result in measurement of significant spectral differences that arise from distinct chemical end-members that also exhibit a clear visual dichotomy in corresponding MAHLI images (VanBommel et al., 2016, VanBommel et al., 2017).

TABLE S3-1. APXS DATA FOR FUNDA, IN NASA PDS ARCHIVES

Funda APXS raster spot	archived data files
1	APB_522598925ESC14090560000_____M1.DAT and APB_522599809ESC14090560000_____M1.DAT
2	APB_522600752ESC14090560000_____M1.DAT and APB_522601636ESC14090560000_____M1.DAT
3	APB_522602580ESC14090560000_____M1.DAT and APB_522603464ESC14090560000_____M1.DAT
4	APB_522604410ESC14090560000_____M1.DAT and APB_522605294ESC14090560000_____M1.DAT
concentrations list	msl_apxs_concentrations_1294_1417.csv

The inferred position of the 4-spot APXS raster at Funda is shown in **Figure S3-1A**. Funda was only in part of the FOV at spots 3 and 4 (**Fig. S3-1A**). To isolate its composition, it, and the bulk gray rock surrounding it (the composite of framework grains, matrix, and cement), were the end-members considered. Visual inspection of MAHLI images of the target area (**Fig. S3-1A**) suggests that additional end-members (i.e., the pebbles) might also contribute to chemical variation between the measured APXS spots. However, the results from APXS indicate that the potential effect is minor given the chemical similarity between the four APXS measurements relative to the difference presented by the white feature. Additionally, of the four spots, only spot 3 provides a unique chemistry, enriched in SO_3 and CaO compared to the other interrogation spots (**Fig. S3-1B**).

Following the approach of VanBommel et al. (2016) and VanBommel et al. (2017), we used MAHLI image center locations to constrain the four APXS FOV locations at Funda (**Fig. S3-1A**). In the software analysis, deviation (lateral translation and rotation) during localization from these fixed positions was permitted but was expected to be minimal given the precision of the robotic arm. For the initial assessment, the end-member chemistry was unrestricted. Via this approach, the chemistry of the white feature converged on $CaSO_4$ but with large uncertainties given the limited spatial coverage within a single APXS FOV. The chemistry of Funda was then fixed as $CaSO_4$ and the localization technique was repeated. The determined location for each raster spot (**Fig. S3-1A**) was within millimeters of the variable feature chemistry localization and had a similar chemical deconvolution analysis χ^2. APXS coverage of Funda is estimated to be 8 ± 3% and 1 ± 1% in spots 3 and 4, respectively. Funda was not present in, and differs from the chemistry of, spots 1 and 2.

As a corollary to the localization and deconvolution approach, we also confirmed that Funda consists of or contains $CaSO_4$ via the techniques of VanBommel et al. (2019a) and VanBommel et al. (2019b). In this analysis, the spot 3 APXS spectrum was compared to a modeled spectrum of *n%* $CaSO_4$ and *(1–n)%* substrate. The substrate chemistry was inferred from an average of spots 1, 2, and 4. Reported APXS chemistry values assume a homogenous sample. As a result, in the case of obvious (in MAHLI images) heterogeneities, matrix effects (such as Ca attenuation inside pure $CaSO_4$ as compared to basalt) can skew the resulting deconvolved chemistry from the theoretical, as was observed in analysis of a pure $CaSO_4$ vein target named Sayunei examined using the APXS on Sol 165 (VanBommel et al., 2016). The spectral modeling algorithm (VanBommel et al., 2019a; VanBommel et al., 2019b) properly handles matrix effects by determining the attenuation cross-sections of each end-member prior to calculating peak areas. From this modeling, the spot 3 spectrum is accurately predicted to be a mixture of the average surrounding substrate and 4 ± 1% pure $CaSO_4$ (**Fig. S3-1C**).

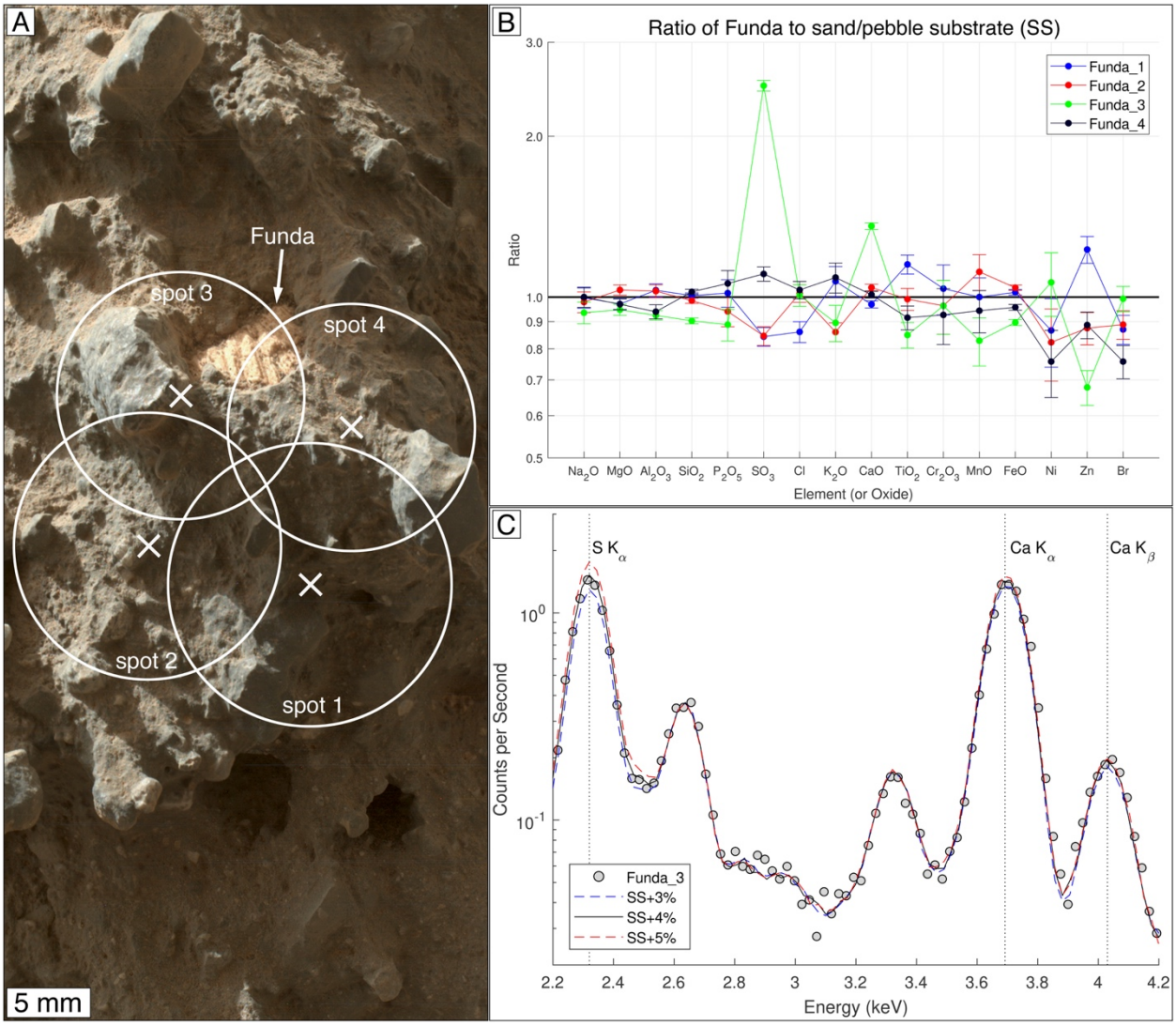

Figure S3-1. APXS observations of Funda; SS refers to the gray sand and pebble clasts which were observed, along with Funda, by the APXS. **(A)** Best (χ^2) fit for the locations for each of the four APXS observation spots at Funda. **(B)** Ratio of APXS-derived elemental composition of Funda to the average deconvolved composition of the gray sand and pebbles (SS) at each observation spot (1–4). Note the relative enrichment of SO_3 and CaO at spot 3 (green). **(C)** Simulated spectra consisting of a mixture of average substrate (SS) plus varying abundance of $CaSO_4$ overlaid with the observed spot 3 (Funda_3, gray dots) spectrum. Good agreement is achieved with 4 ± 1% $CaSO_4$.

REFERENCES CITED IN THIS SUPPLEMENT

Collins, C.L., and Robinson, M.L., 2013, Accuracy analysis and validation of the Mars Science Laboratory (MSL) robotic arm: Proceedings of the American Society of Mechanical Engineers Mechanisms and Robotics Conference 37, https://doi.org/10.1115/DETC2013-13034.

Gellert, R., Clark, B.C. III, and the MSL and MER Science Teams, 2015, In situ compositional measurements of rocks and soils with the Alpha Particle X-Ray Spectrometer on NASA's Mars rovers: Elements, v. 11, no. 1, p. 39–44, https://doi.org/10.2113/gselements.11.1.39.

Gellert, R., Rieder, R., Brückner, J., Clark, B.C., Dreibus, G., Klingelhöfer, G., Lugmair, G., Ming, D.W., Wänke, H., Yen, A., Zipfel, J., and Squyres, S.W., 2006, Alpha Particle X-Ray Spectrometer (APXS): Results from Gusev crater and calibration report: Journal of Geophysical Research, Planets, v. 111, E02S05, https://doi.org/10.1029/2005JE002555.

VanBommel, S.J., Gellert, R., Berger, J.A., Campbell, J.L., Thompson, L.M., Edgett, K.S., McBride, M.J., Minitti, M.E., Pradler, I., and Boyd, N.I., 2016, Deconvolution of distinct lithology chemistry through oversampling with the Mars Science Laboratory Alpha Particle X-ray Spectrometer: X-Ray Spectrometry, v. 45, p. 155–161, https://doi.org/10.1002/xrs.2681.

VanBommel, S.J., Gellert, R., Berger, J.A., Thompson, L.M., Edgett, K.S., McBride, M.J., Minitti, M.E., Boyd, N.I., and Campbell, J.L., 2017, Modeling and mitigation of sample relief effects applied to chemistry measurements by the Mars Science Laboratory Alpha Particle X-ray Spectrometer: X-Ray Spectrometry, v. 46, p. 229–236, https://doi.org/10.1002/xrs.2755.

VanBommel, S.J., Gellert, R., Berger, J.A., Yen, A.S., and Boyd, N.I., 2019a, Mars Science Laboratory Alpha Particle X-ray Spectrometer trace elements: Situational sensitivity to Co, Ni, Cu, Zn, Ga, Ge, and Br: Acta Astronautica, v. 165, p. 32–42, https://doi.org/10.1016/j.actaastro.2019.08.026.

VanBommel, S.J., Gellert, R., Boyd, N.I., and Hanania, J.U., 2019b, Empirical simulations for further characterization of the Mars Science Laboratory Alpha Particle X-ray Spectrometer: An Introduction to the ACES program: Nuclear Instruments and Methods in Physics Research, Section B, Beam Interactions with Materials and Atoms, v. 441, p. 79–87, https://doi.org/10.1016/j.nimb.2018.12.040.